Metastability of Liquid Water Freezing into Ice VII Under Dynamic Compression

M. C. Marshall,[1,2] M. Millot,[2] D. E. Fratanduono,[2] D. M. Sterbentz,[2,3] P. C. Myint,[2] J. L. Belof,[2] Y.-J. Kim,[2] F. Coppari,[2] S. J. Ali,[2] J. H. Eggert,[2] R. F. Smith,[2] and J. M. McNaney[2]

[1]Laboratory for Laser Energetics, University of Rochester
[2]Lawrence Livermore National Laboratory
[3]University of California Davis

Dynamic compression is often used to create the nonequilibrium conditions needed to study metastability and kinetic effects in materials as they undergo phase transitions.[1,2] In particular, the pressure-induced phase transformation of liquid water solidifying into ice VII has been the focus of many experimental and theoretical works.[3–9] Under rapid submillisecond compression, the liquid phase can persist metastably well into pressure–temperature conditions where ice VII is the stable phase.[3–5] Previous experimental studies found that liquid water can remain metastable to at least 7 GPa— ~5 GPa higher than expected based on the equilibrium phase diagram—before homogeneously freezing into ice VII when quasi-isentropically (ramp) compressed over hundreds of nanoseconds.[3–5] This work ramp compresses liquid water over the highest compression rates to date (up to ~3 GPa/ns) to further investigate its metastability limit.

Water was ramp compressed into the ice VII phase in experiments at the Omega Laser Facility.[10,11] The liquid–ice VII phase transition in a thin water layer, sandwiched between a baseplate and a sapphire or quartz window, was diagnosed using a velocity interferometer system for any reflector (VISAR).[12] Since ice VII is ~5% more dense than liquid water at the phase transition conditions, the volume of the thin water layer abruptly decreases during the phase transition (~1-ns duration), which alleviates pressure on the water/window interface despite the continuously increasing pressure drive.[3–5] The VISAR records a corresponding dip in the water/window interface velocity, which we interpret as the liquid freezing into ice VII (Fig. 1).

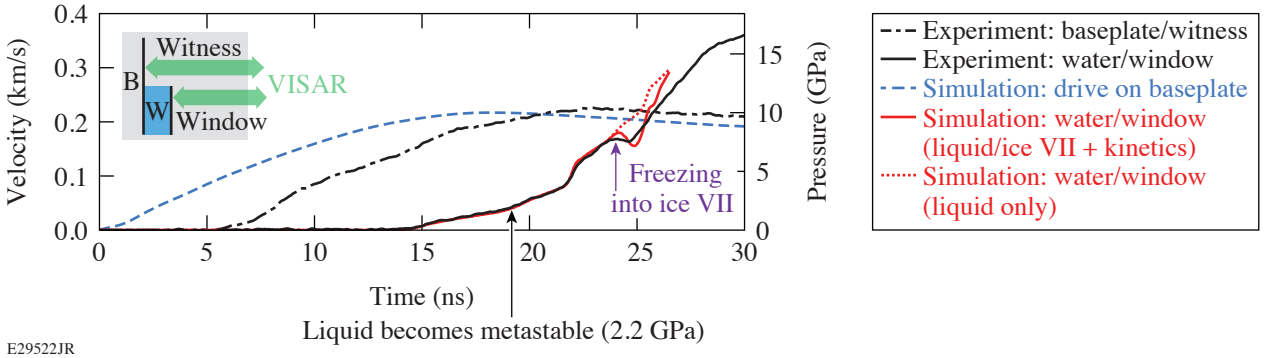

Figure 1
Interface velocities and corresponding pressures (applicable to all curves) from experiment shot 29419 and the post-shot simulations. An inset of the target components relevant to the experimental measurements and simulations is shown, where "B" is the sapphire baseplate, "W" is the water, "Witness" is the sapphire witness, and "Window" is the sapphire window. The VISAR probes a reflective Al coating at the baseplate/witness and water/window interfaces to measure their velocities. A dip in the water/window interface pressure, resulting from the liquid water freezing into the ~5%-more-dense ice VII phase, is observed near 24 ns and 7.5 GPa in the experiment and simulation using the liquid/ice VII equation of state and classical nucleation theory–based kinetics model.

Water was compressed at rates spanning from 0.2 to 3 GPa/ns over 15 experiments, where the loading rate was varied by changing the laser intensity, the baseplate thickness, and the window material (e.g., the lower impedance of quartz compared to sapphire leads to shallower ramp compression profiles) (Fig. 2). We find that the liquid–ice VII freezing pressure, defined as the pressure in the liquid at the peak velocity before the dip, for water compressed on the principal isentrope increases with compression rate to at least ~8 GPa [Fig. 2(a)]. We observed freezing at pressures as high as ~9 GPa; however, additional heating of <8 K above the principal isentrope cannot be ruled out, which could further raise the freezing pressure.[4] These results indicate that liquid water can exist to at least ~3.5× higher pressure than the onset of metastability (2.2 GPa) (Ref. 9) and that the metastability limit is at least ~11% higher than previously reported.[3–5] Agreement between data at 0.1 to 0.3 GPa/ns in Fig. 2(a) from this work (Omega), Dolan *et al.* (Z),[3] and Nissen *et al.* (Thor)[4] (all room temperature), obtained using different target component materials, suggests that ice VII is nucleated homogeneously in the bulk and not heterogeneously at the various window or baseplate surfaces.

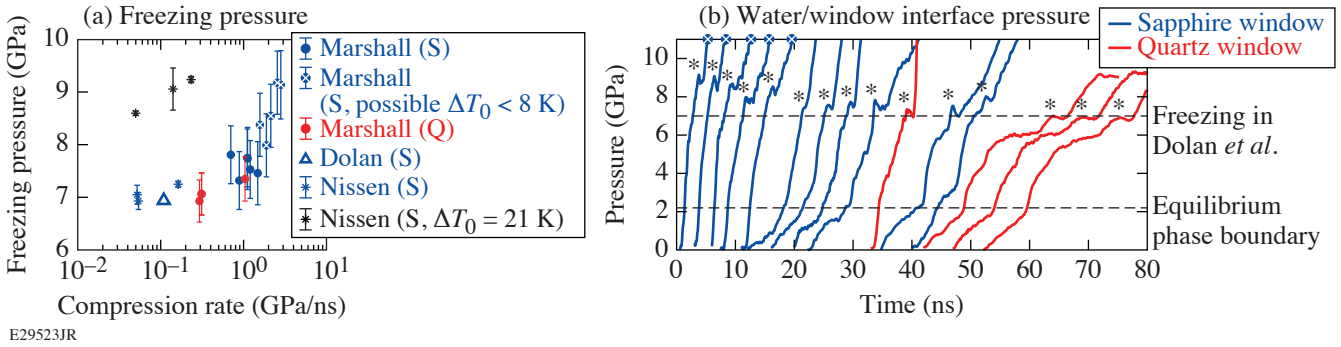

Figure 2
(a) Liquid–ice VII freezing pressure versus compression rate [(defined from 2.2 GPa ([onset of metastability)] to the freezing pressure]) and (b) pressure histories of the water/window interface for all shots ordered by decreasing compression rate and shifted in time for clarity. In the legend of (a), S and Q denote sapphire and quartz windows, respectively, and ΔT_0 is the initial temperature increase above the principal isentrope. Asterisks in (b) mark the pressure relaxation interpreted as freezing.

Our experimental results can be reproduced in hydrodynamic simulations (*ARES*) using a kinetics model (SAMSA)[13] that, remarkably at these extreme conditions, is fundamentally based on classical nucleation theory (CNT).[8] The baseplate/water/window portions of the target were simulated using a pressure input on the front baseplate surface that were determined from the shot-specific sapphire "witness" measurements adjacent to the water layer. The same pressure relaxation at the water/window interface observed in the experiment is also observed in the simulation using the CNT-based kinetics model[8] and a multiphase equation of state (EOS) for the liquid and ice VII phases[14] (Fig. 1). This pressure relaxation is concurrent with the onset and completion of freezing in the simulations. The "null case" of no phase transition, represented by using only the liquid EOS, does not show the dip in the water/window interface pressure, suggesting that the dip observed in the experiment is indeed the result of freezing and not wave reverberations within the target.

The experiments reported here are at the frontier of using experimental ultrafast science to explore metastability and kinetics associated with phase transitions. It is remarkable that recent theoretical and numerical advances provide a detailed understanding of the observed phenomena, while relying on the fundamentally simple picture of homogeneous nucleation using CNT. This could have implications for our general understanding of phase transformations at extreme conditions.

This material is based upon work supported by the Department of Energy National Nuclear Security Administration under Award Number DE-NA0003856, the University of Rochester, and the New York State Energy Research and Development Authority. This work was performed under the auspices of the U.S. Department of Energy by Lawrence Livermore National Laboratory under Contract No. DE-AC52-07NA27344.

1. R. F. Smith *et al.*, Phys. Rev. Lett. **101**, 065701 (2008).
2. S. J. Tracy, S. J. Turneaure, and T. S. Duffy, Sci. Adv. **6**, eabb3913 (2020).
3. D. H. Dolan *et al.*, Nat. Phys. **3**, 339 (2007).
4. E. J. Nissen and D. H. Dolan, J. Appl. Phys. **126**, 015903 (2019).
5. M. Bastea *et al.*, Phys. Rev. B **75**, 172104 (2007).
6. A. E. Gleason *et al.*, Phys. Rev. Lett. **119**, 025701 (2017).
7. P. C. Myint *et al.*, Phys. Rev. Lett. **121**, 155701 (2018).
8. D. M. Sterbentz *et al.*, J. Chem. Phys. **151**, 164501 (2019).
9. P. C. Myint and J. L. Belof, J. Phys.: Condens. Matter **30**, 233002 (2018).
10. T. R. Boehly *et al.*, Opt. Commun. **133**, 495 (1997).
11. D. D. Meyerhofer *et al.*, J. Phys.: Conf. Ser. **244**, 032010 (2010).
12. P. M. Celliers *et al.*, Rev. Sci. Instrum. **75**, 4916 (2004).
13. P. C. Myint *et al.*, AIP Adv. **10**, 125111 (2020).
14. P. C. Myint, L. X. Benedict, and J. L. Belof, J. Chem. Phys. **147**, 084505 (2017).